

Table of Content

Figure S1.	ATR-FTIR spectra of (A) 1 , (B) 2 , (C) 3 , and (D) 4 in the solid form.
Figure S2.	UV-Vis spectra of 1-4 (50 μ M) in chloroform at room temperature.
Table S1.	Experimentally determined LogP values for 1-4 .
Figure S3.	UV-Vis spectrum of 1 (50 μ M) in PBS:DMSO (200:1) over the course of 24 h at 37 °C.
Figure S4.	UV-Vis spectrum of 3 (50 μ M) in PBS:DMSO (200:1) over the course of 24 h at 37 °C.
Figure S5.	UV-Vis spectrum of 2 (50 μ M) in PBS:DMSO (200:1) over the course of 24 h at 37 °C.
Figure S6.	UV-Vis spectrum of 4 (50 μ M) in PBS:DMSO (200:1) over the course of 24 h at 37 °C.
Figure S7.	UV-Vis spectrum of 1 in mammary epithelial cell growth medium (MEGM):DMSO (200:1) over the course of 24 h at 37 °C.
Figure S8.	UV-Vis spectrum of 3 in mammary epithelial cell growth medium (MEGM):DMSO (200:1) over the course of 24 h at 37 °C.
Figure S9.	UV-Vis spectrum of 2 in mammary epithelial cell growth medium (MEGM):DMSO (200:1) over the course of 24 h at 37 °C.
Figure S10.	UV-Vis spectrum of 4 in mammary epithelial cell growth medium (MEGM):DMSO (200:1) over the course of 24 h at 37 °C.
Figure S11.	Representative dose-response curves for the treatment of HMLER and HMLER-shEcad cells with 1 .
Figure S12.	Representative dose-response curves for the treatment of HMLER and HMLER-shEcad cells with 3 .
Figure S13.	Chemical structures of the copper(II)-3,4,7,8-tetramethyl-1,10-phenanthroline complexes containing the non-steroidal anti-inflammatory drugs (NSAIDs), naproxen and indomethacin, Cu-1 and Cu-3 .
Figure S14.	Representative dose-response curves for the treatment of HMLER and HMLER-shEcad cells with $\text{NiCl}_2 \cdot 6\text{H}_2\text{O}$.
Figure S15.	Representative dose-response curves for the treatment of MCF10A cells with 1 and 3 .
Figure S16.	Quantification of mammosphere formation with HMLER-shEcad cells untreated and treated with $\text{NiCl}_2 \cdot 6\text{H}_2\text{O}$ (at 2 μ M for 5 days). Error bars = SD.
Figure S17.	Representative bright-field images (x 10) of the mammospheres in the absence and presence of $\text{NiCl}_2 \cdot 6\text{H}_2\text{O}$ (at 2 μ M for 5 days).
Figure S18.	Representative dose-response curves for the treatment of HMLER-shEcad mammospheres with 1 , 3 , $\text{NiCl}_2 \cdot 6\text{H}_2\text{O}$, or naproxen after 5 days incubation.
Figure S19.	Representative histograms displaying the green fluorescence emitted by anti-COX-2 Alexa Fluor 488 nm antibody-stained HMLER-shEcad cells treated with LPS (2.5 μ M) for 24 h (red) followed by 72 h in media containing naproxen (20 μ M, blue) or indomethacin (20 μ M, orange).
Figure S20.	Representative histograms displaying the green fluorescence emitted by anti-COX-2 Alexa Fluor 488 nm antibody-stained HMLER-shEcad cells treated with LPS (2.5 μ M) for 24 h (red) followed by 72 h in media containing $\text{NiCl}_2 \cdot 6\text{H}_2\text{O}$ (20 μ M, blue).

- Figure S21.** Representative dose-response curves for the treatment of HMLER-shEcad cells with **1** after 72 incubation in the presence and absence of PGE2 (20 μ M).
- Figure S22.** Representative dose-response curves for the treatment of HMLER-shEcad cells with **1** after 72 incubation in the presence and absence of IM-54 (10 μ M), necrostatin-1 (20 μ M), or dabrafenib (20 μ M).
- Figure S23.** Representative dose-response curves for the treatment of HMLER-shEcad cells with **3** after 72 incubation in the presence and absence of IM-54 (10 μ M), necrostatin-1 (20 μ M), or dabrafenib (20 μ M).
- Figure S24.** Graphical representation of the IC₅₀ values of **1** against HMLER-shEcad cells in the absence and presence of IM-54 (10 μ M), necrostatin-1 (20 μ M), or dabrafenib (10 μ M). Error bars represent standard deviations and Student t-test, * = $p < 0.05$.

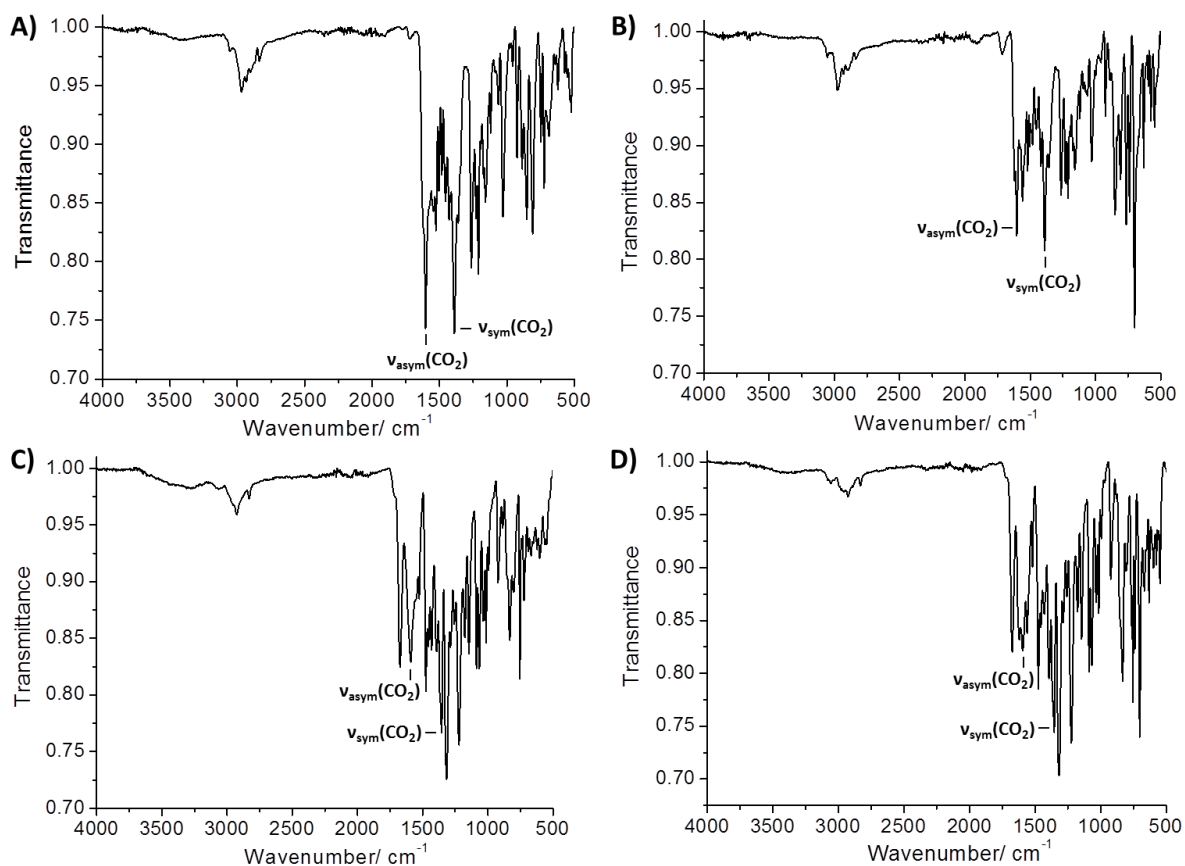


Figure S1. ATR-FTIR spectra of (A) **1**, (B) **2**, (C) **3**, and (D) **4** in the solid form.

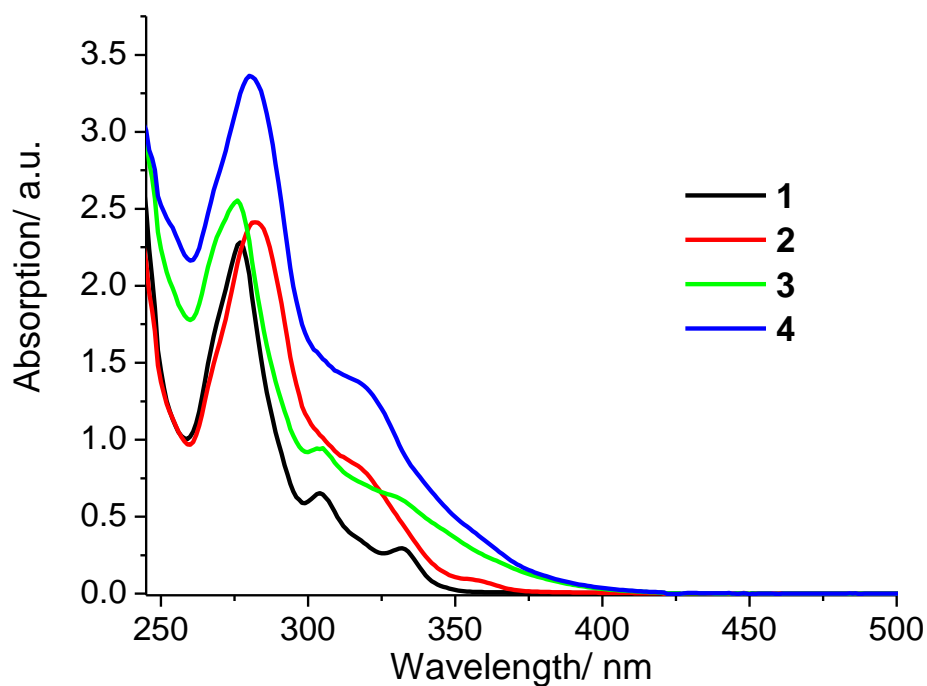


Figure S2. UV-Vis spectra of **1-4** (50 μM) in chloroform at room temperature.

Table S1. Experimentally determined LogP values for **1-4**.

Metal complex	LogP
1	0.63 ± 0.05
2	1.21 ± 0.11
3	0.96 ± 0.13
4	1.52 ± 0.14

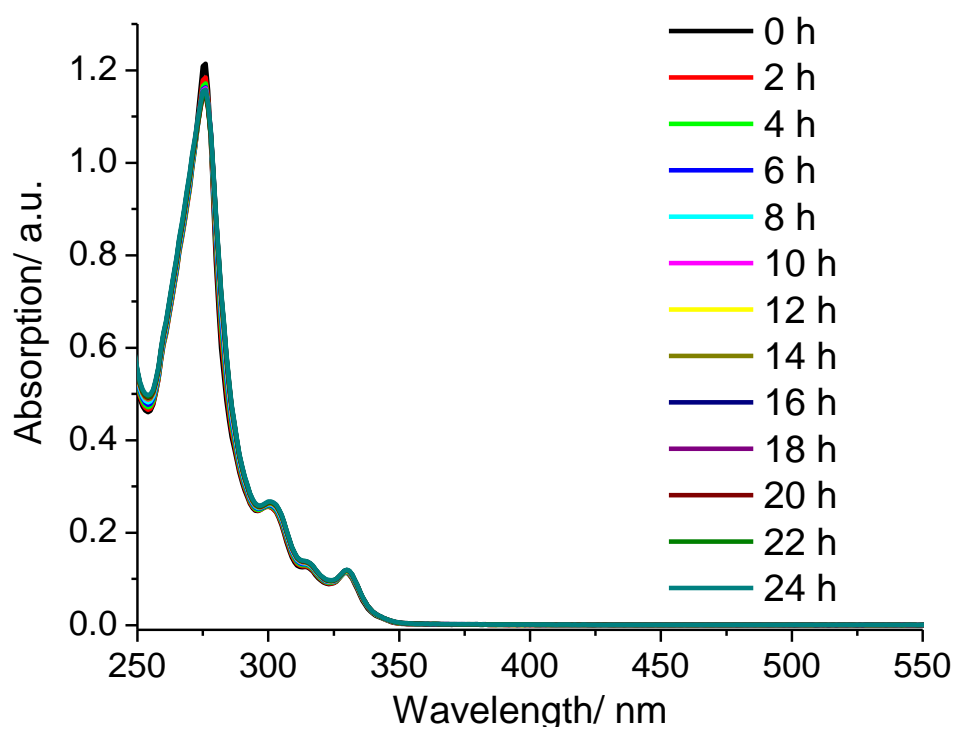


Figure S3. UV-Vis spectrum of **1** (50 μ M) in PBS:DMSO (200:1) over the course of 24 h at 37 $^{\circ}$ C.

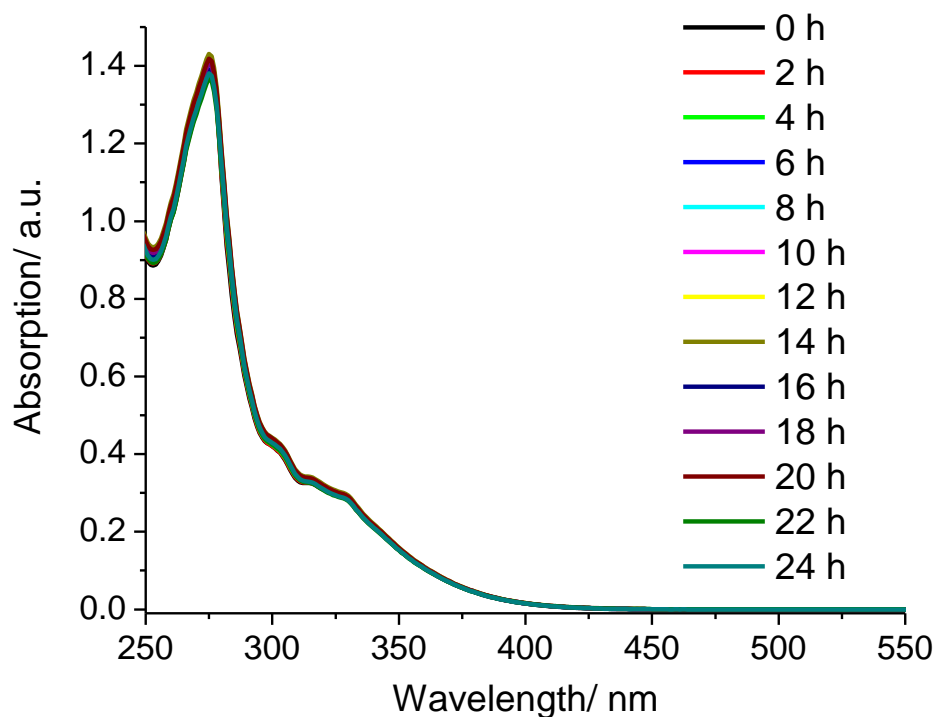


Figure S4. UV-Vis spectrum of **3** (50 μM) in PBS:DMSO (200:1) over the course of 24 h at 37 $^{\circ}\text{C}$.

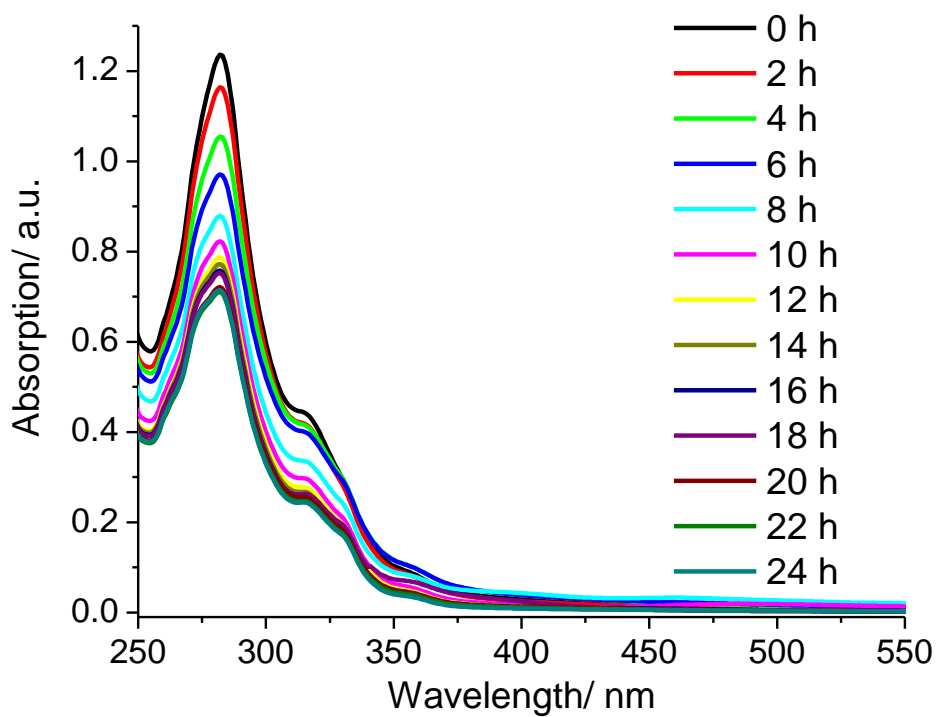


Figure S5. UV-Vis spectrum of **2** (50 μM) in PBS:DMSO (200:1) over the course of 24 h at 37 $^{\circ}\text{C}$.

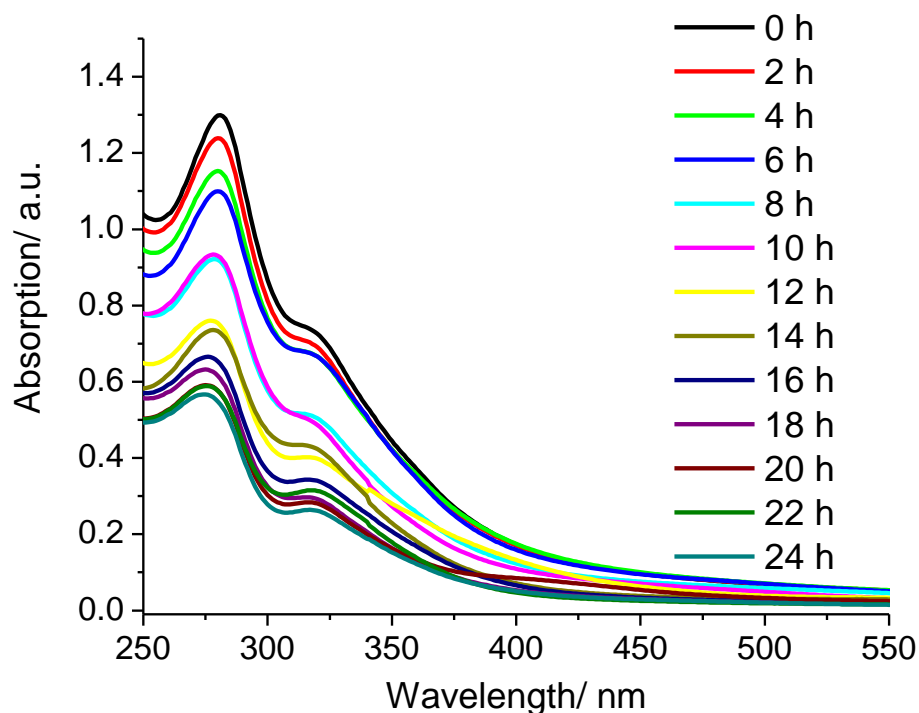


Figure S6. UV-Vis spectrum of **4** (50 μ M) in PBS:DMSO (200:1) over the course of 24 h at 37 $^{\circ}$ C.

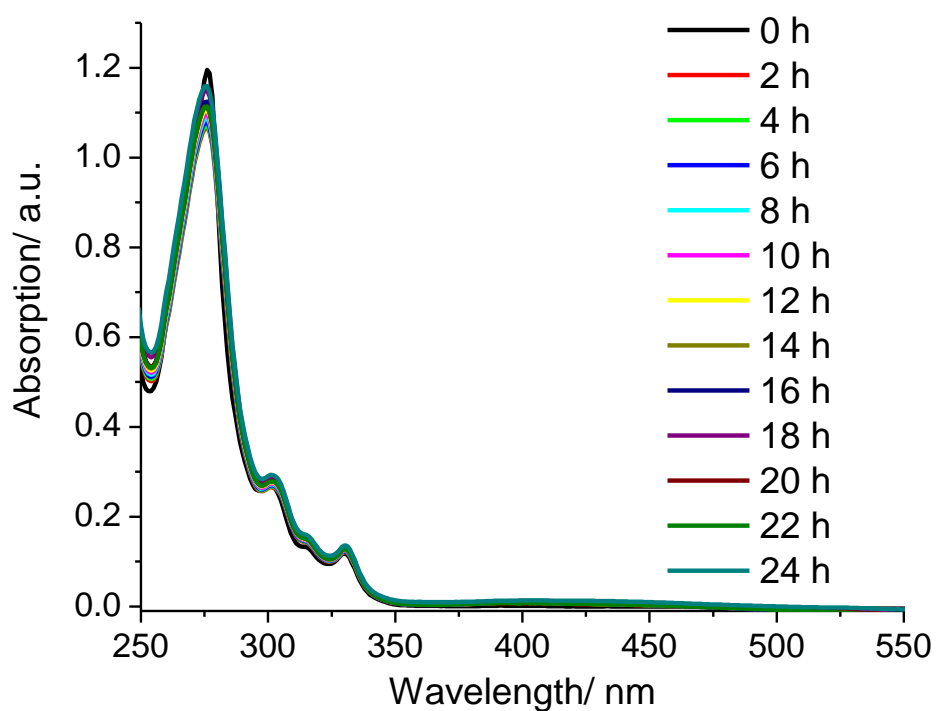


Figure S7. UV-Vis spectrum of **1** in mammary epithelial cell growth medium (MEGM):DMSO (200:1) over the course of 24 h at 37 $^{\circ}$ C.

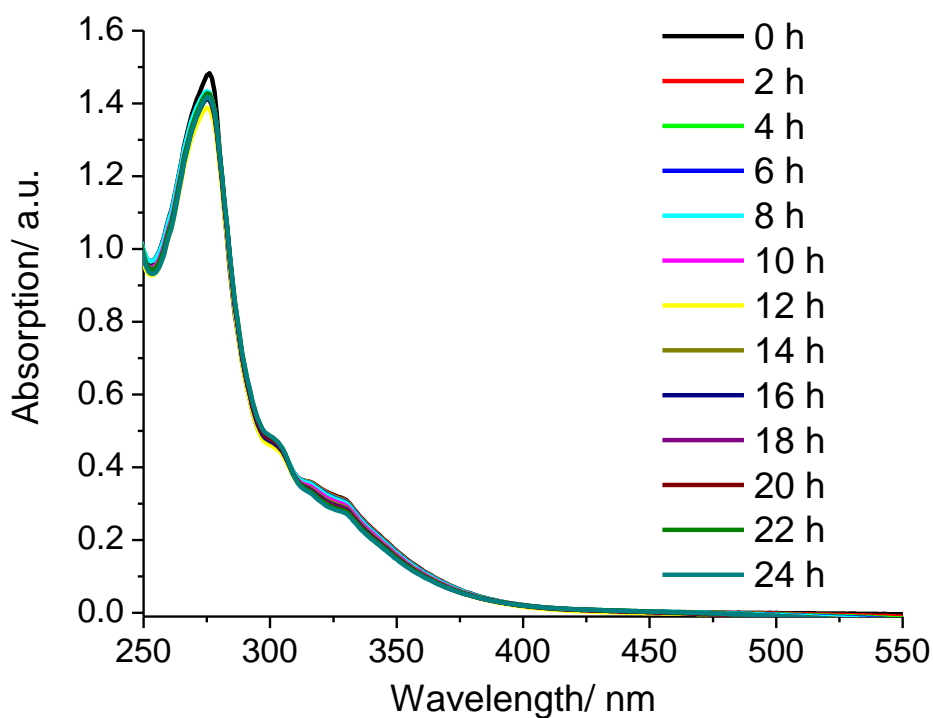


Figure S8. UV-Vis spectrum of **3** in mammary epithelial cell growth medium (MEGM):DMSO (200:1) over the course of 24 h at 37 °C.

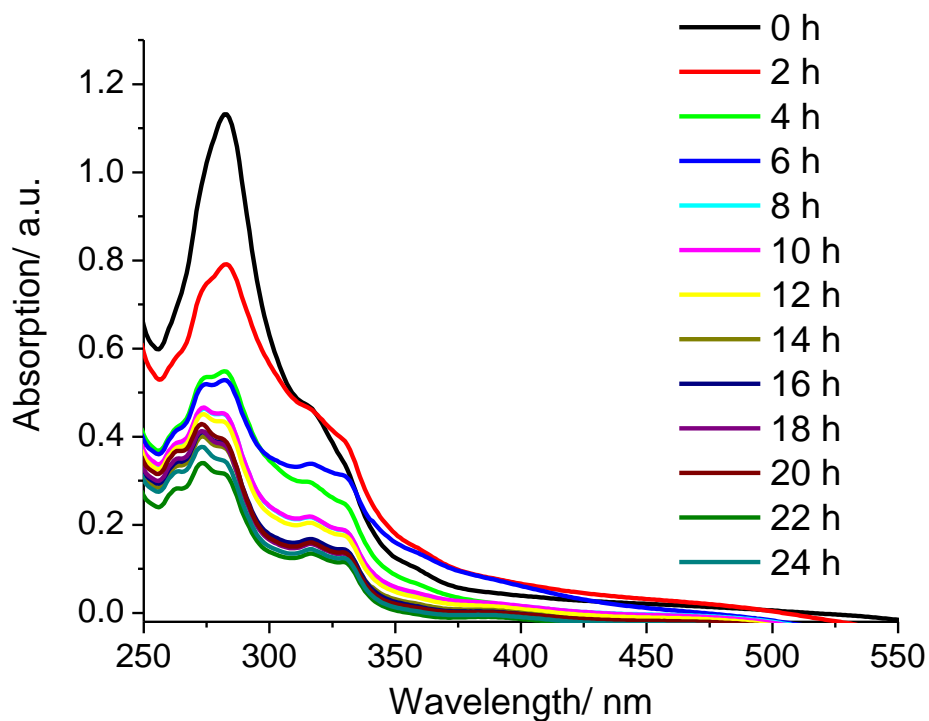


Figure S9. UV-Vis spectrum of **2** in mammary epithelial cell growth medium (MEGM):DMSO (200:1) over the course of 24 h at 37 °C.

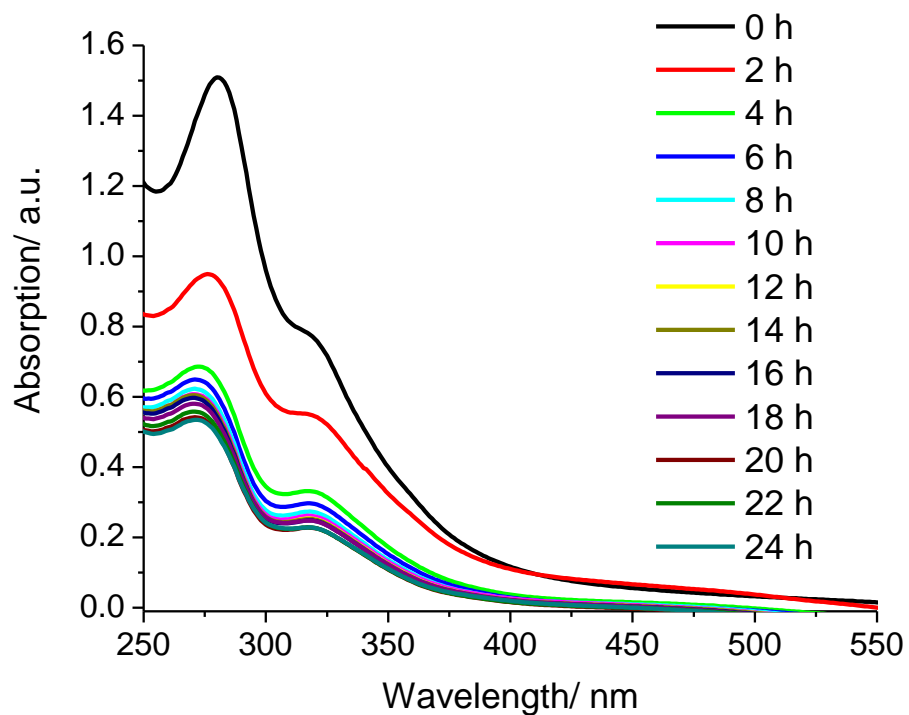


Figure S10. UV-Vis spectrum of **4** in mammary epithelial cell growth medium (MEGM):DMSO (200:1) over the course of 24 h at 37 °C.

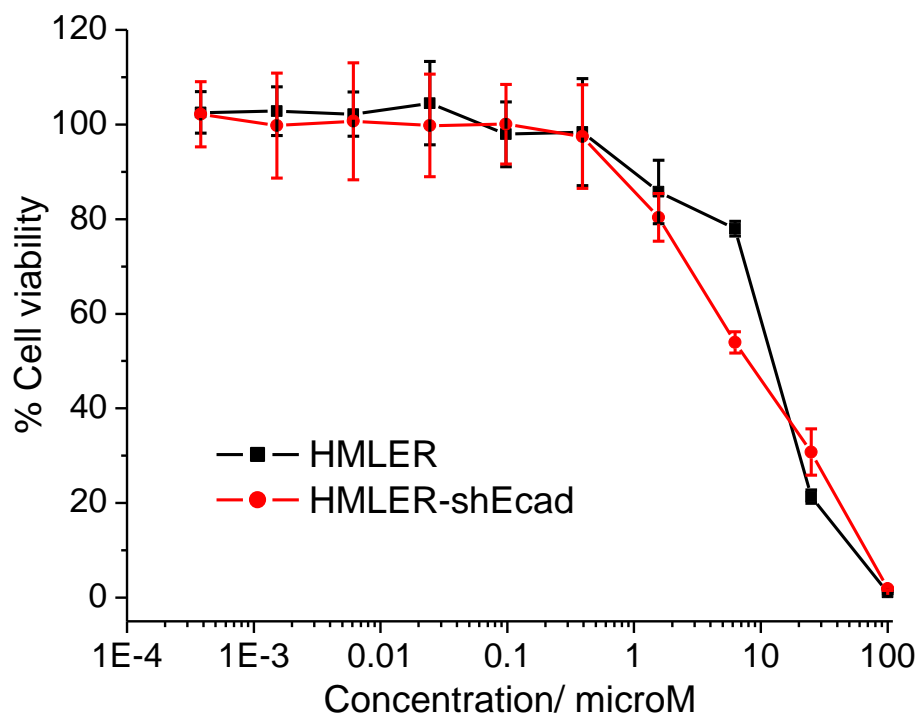


Figure S11. Representative dose-response curves for the treatment of HMLER and HMLER-shEcad cells with **1**.

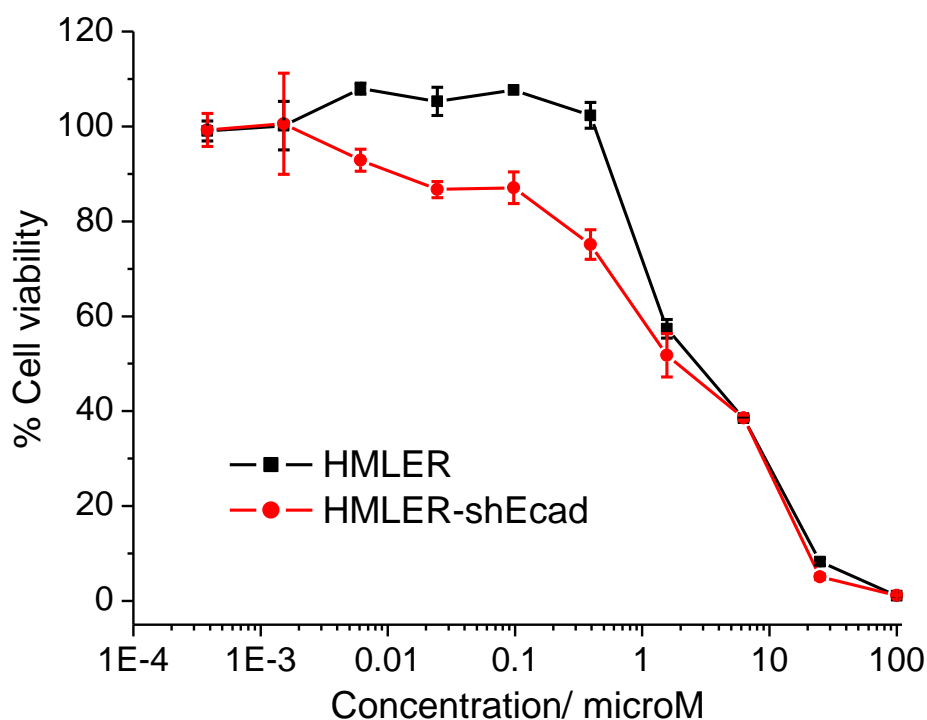


Figure S12. Representative dose-response curves for the treatment of HMLER and HMLER-shEcad cells with **3**.

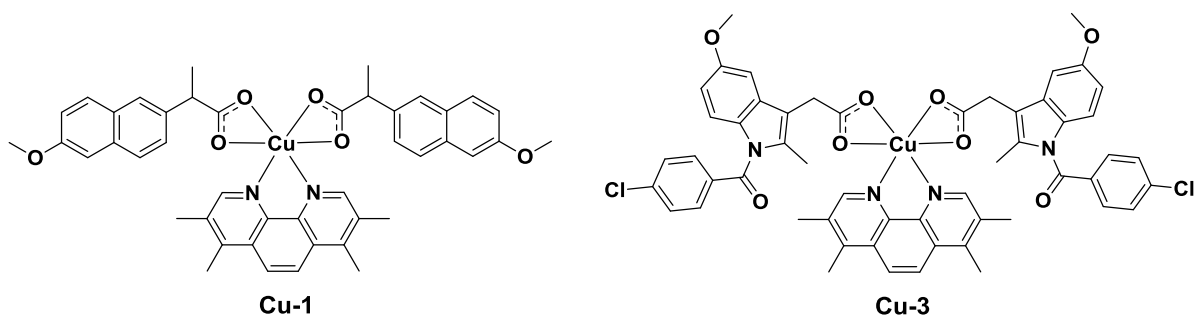


Figure S13. Chemical structures of the copper(II)-3,4,7,8-tetramethyl-1,10-phenanthroline complexes containing the non-steroidal anti-inflammatory drugs (NSAIDs), naproxen and indomethacin, **Cu-1** and **Cu-3**.

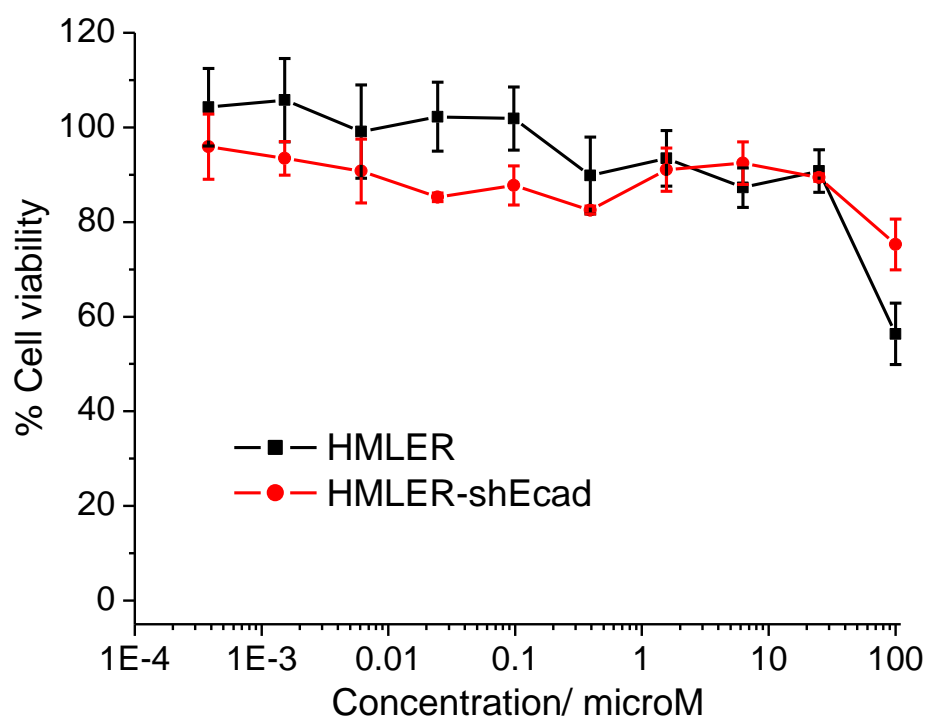


Figure S14. Representative dose-response curves for the treatment of HMLER and HMLER-shEcad cells with $\text{NiCl}_2 \cdot 6\text{H}_2\text{O}$.

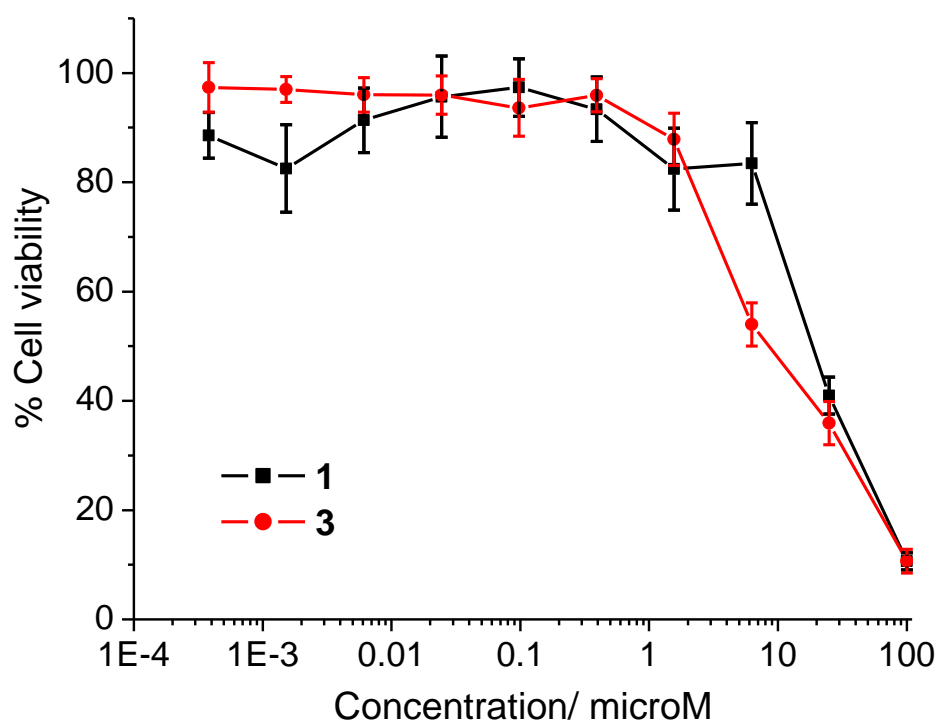


Figure S15. Representative dose-response curves for the treatment of MCF10A cells with 1 and 3.

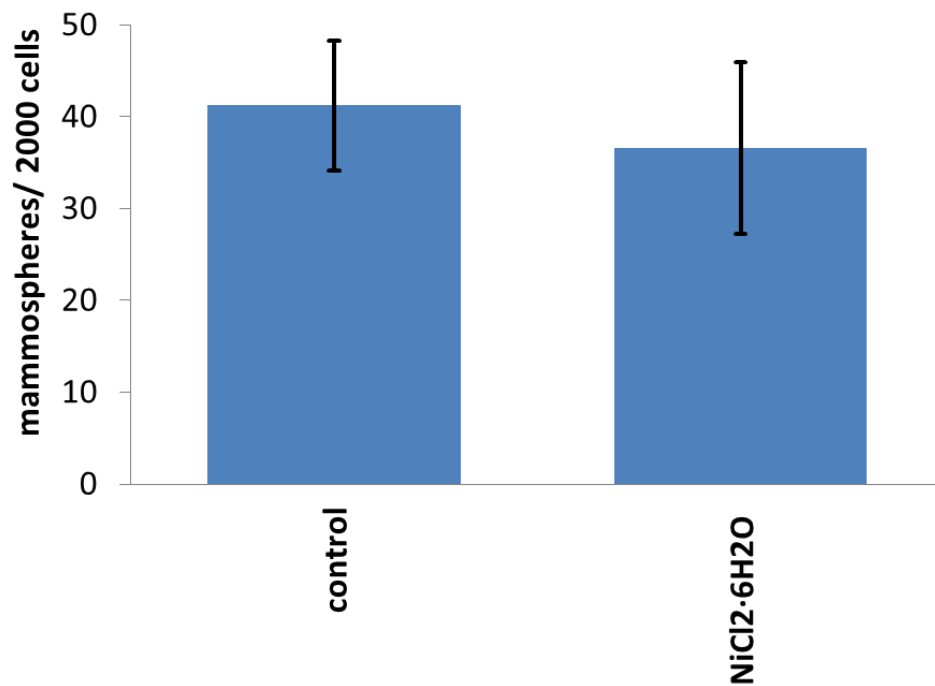


Figure S16. Quantification of mammosphere formation with HMLER-shEcad cells untreated and treated with NiCl₂·6H₂O (at 2 μ M for 5 days). Error bars = SD.

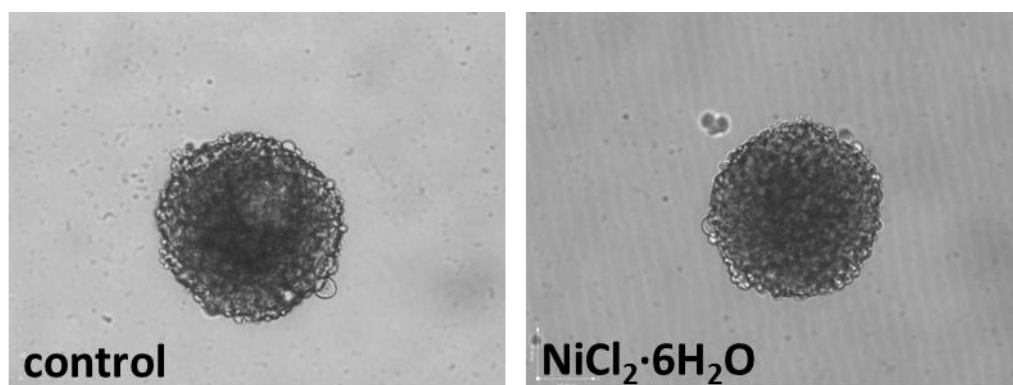


Figure S17. Representative bright-field images (x 10) of the mammospheres in the absence and presence of NiCl₂·6H₂O (at 2 μ M for 5 days).

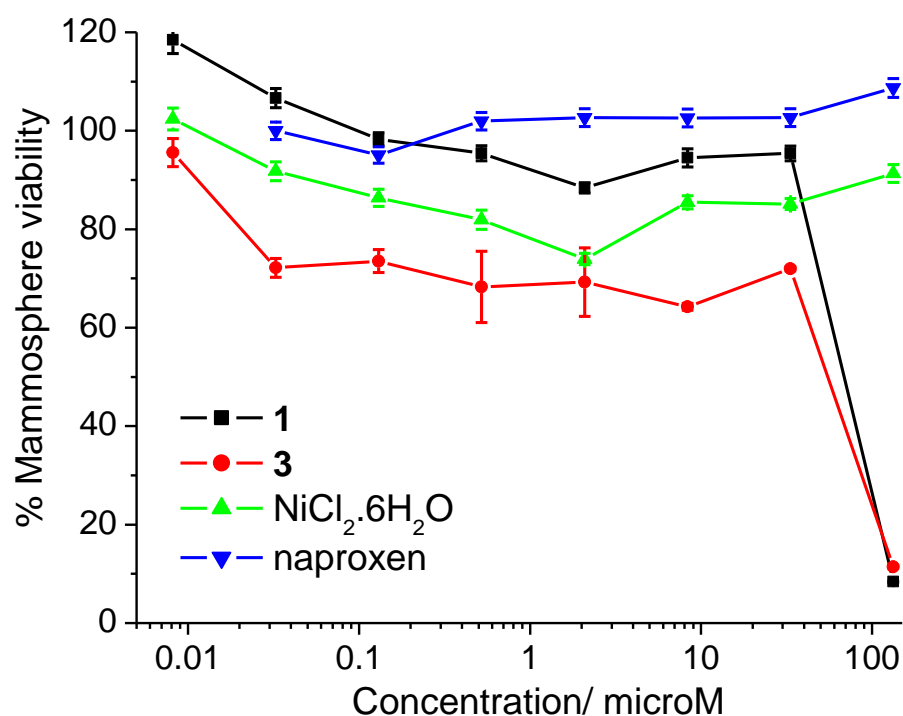


Figure S18. Representative dose-response curves for the treatment of HMLER-shEcad mammospheres with **1**, **3**, NiCl₂·6H₂O, or naproxen after 5 days incubation.

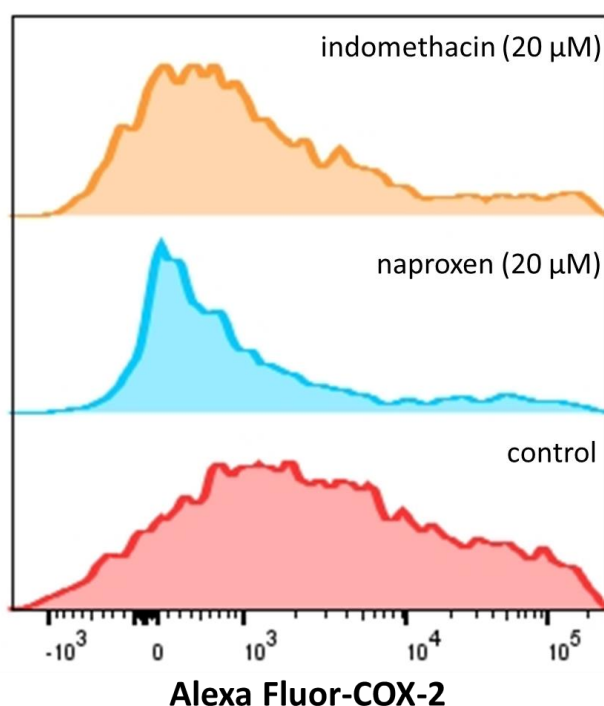


Figure S19. Representative histograms displaying the green fluorescence emitted by anti-COX-2 Alexa Fluor 488 nm antibody-stained HMLER-shEcad cells treated with LPS (2.5 μM) for 24 h (red) followed by 72 h in media containing naproxen (20 μM, blue) or indomethacin (20 μM, orange).

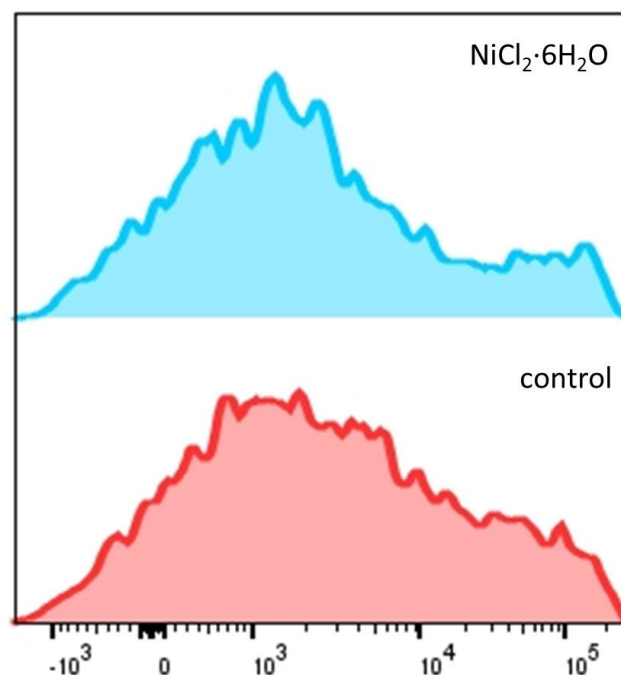


Figure S20. Representative histograms displaying the green fluorescence emitted by anti-COX-2 Alexa Fluor 488 nm antibody-stained HMLER-shEcad cells treated with LPS (2.5 μ M) for 24 h (red) followed by 72 h in media containing $\text{NiCl}_2 \cdot 6\text{H}_2\text{O}$ (20 μ M, blue).

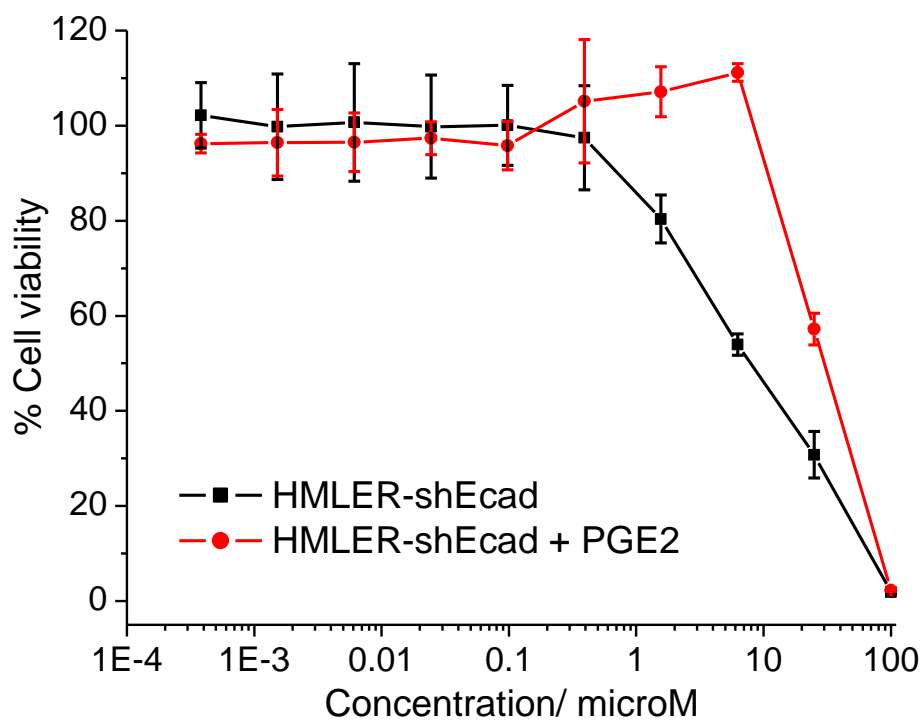


Figure S21. Representative dose-response curves for the treatment of HMLER-shEcad cells with **1** after 72 incubation in the presence and absence of PGE2 (20 μ M).

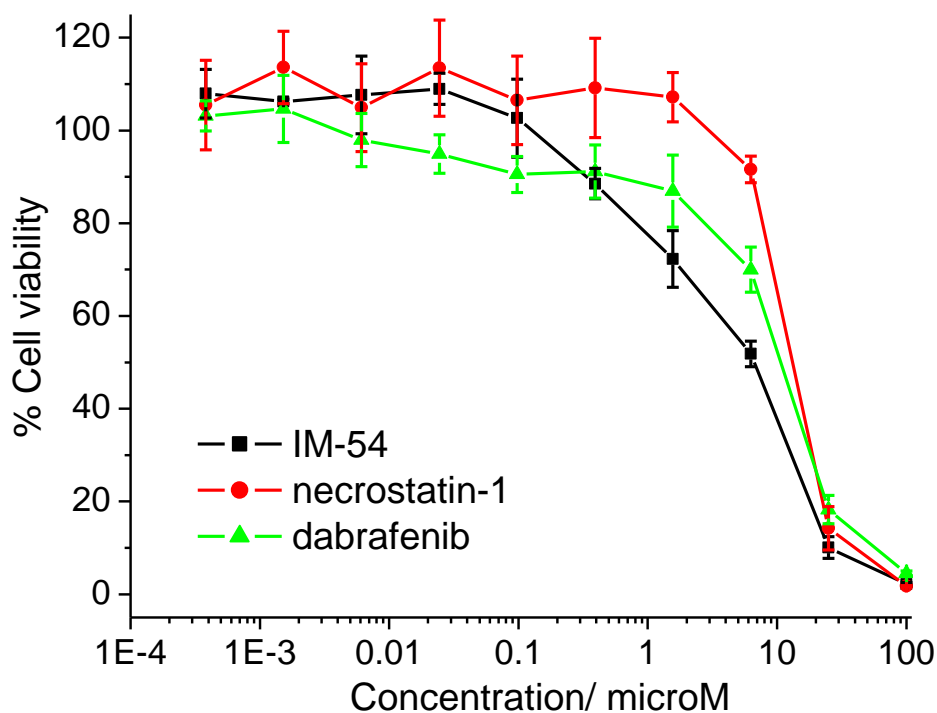


Figure S22. Representative dose-response curves for the treatment of HMLER-shEcad cells with **1** after 72 incubation in the presence and absence of IM-54 (10 µM), necrostatin-1 (20 µM), or dabrafenib (20 µM).

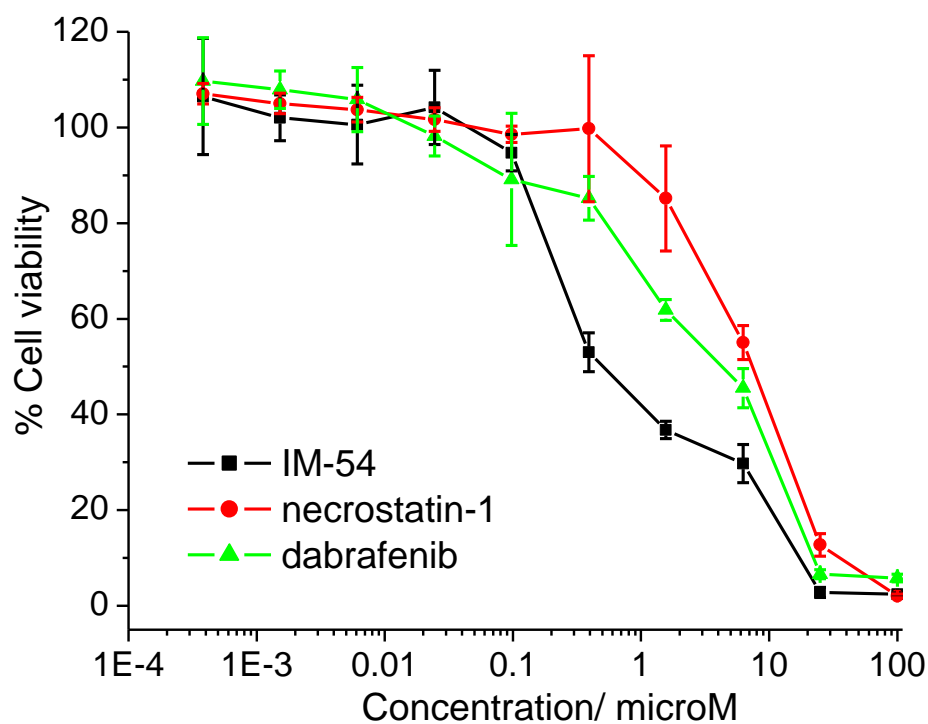


Figure S23. Representative dose-response curves for the treatment of HMLER-shEcad cells with **3** after 72 incubation in the presence and absence of IM-54 (10 µM), necrostatin-1 (20 µM), or dabrafenib (20 µM).

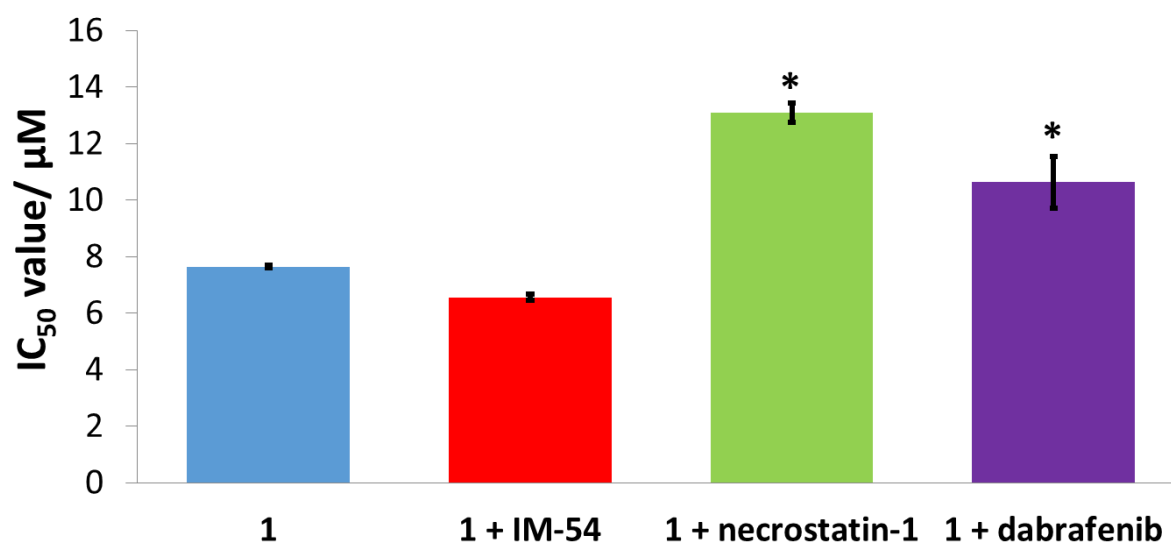


Figure S24. Graphical representation of the IC₅₀ values of **1** against HMLER-shEcad cells in the absence and presence of IM-54 (10 μM), necrostatin-1 (20 μM), or dabrafenib (10 μM). Error bars represent standard deviations and Student t-test, * = $p < 0.05$.